DAMAGE DETECTION ON COOLING TOWER SHELL BASED ON MODEL TEXTURES

David Zahradník and Filip Roučka

Czech Technical University in Prague, Faculty of Civil Engineering, Department of Geomatics, Thákurova 7, Praha 6, Czech Republic; david.zahradnik@fsv.cvut.cz

ABSTRACT

Ensuring the structural integrity of cooling towers is paramount for safety and efficient operation. This paper presents a novel approach for detecting damage on cooling tower shells, utilising textures derived from laser scanning and close-range photogrammetry. The proposed method delves beyond the limitations of solely relying on colour information by harnessing the rich details embedded in various textures, including diffuse, normal, displacement, and occlusion. The study demonstrates the efficacy of this approach for identifying significant concrete damage. A Convolutional Neural Network (CNN) trained on diffuse textures successfully detects high damage instances with minimal misdetection. However, accurately pinpointing low damage, often manifesting as subtle cracks, and mimicking other patterns like air pores, ribbing, and colour variations, presents a formidable challenge. To tackle this challenge, the authors introduce a novel "composed raster layer" that merges information from multiple textures. This pre-processed layer amplifies the visual cues associated with low damage, facilitating its differentiation from similar patterns. While the current implementation employing multi-resolution segmentation and rule-based classification exhibits promising results, further optimization is acknowledged to refine the accuracy of low damage detection. The successful application of textures commonly used in rendering techniques underscores their remarkable potential for enhancing damage detection in civil engineering applications. While acknowledging limitations such as the analysis of a single cooling tower and the reliance on specific software for damage detection, the study proposes future research directions. This research holds significant implications for the field of civil engineering by offering a promising approach for automated and efficient damage detection on cooling tower shells.

KEYWORDS

Cooling tower, Texture, Diffuse, Normal, Displacement, Concrete damage, CNN, UAV

INTRODUCTION

Over the past decade, interest in UAV-sourced data and Structure from Motion (SfM) photogrammetry has surged, transforming aerial remote sensing and mapping. Unmanned Aerial Vehicles (UAVs) represent one of the fastest-growing sectors across various industries including construction, industry, forestry, and ecology, with their applications continually expanding [1]. UAVs play a crucial role in documenting cultural heritage sites, offering a unique perspective and detailed imaging capabilities that aid in preservation efforts [2-4]. The increased availability of UAVs with onboard GNSS RTK offers a promising alternative to georeferencing using ground control points (GCPs), although systematic elevation errors persist [5-6]. Their ability to capture high-resolution imagery provides valuable insights into vegetation health, growth patterns, and environmental changes over time. This versatility underscores the wide-ranging utility of UAVs in ecological research and management practices.

Cooling towers are heat rejection devices used to transfer waste heat from the production process in power, chemical or nuclear plants. The hot water is transferred to air spray and sprayed

on inlet filling where it is cooled and collected in a cold-water basin. Multiple types of cooling towers exist, including the smaller force draft cooling tower, which is box-shaped and uses a propeller within the tower to provide an airflow for the cooling process. The second type of cooling tower is designed in the shape of a hyperboloid and utilises a natural air draft for cooling [7-8].

The design of the hyperbolic cooling tower includes the primary parameters of the tower: height, outlet radius, inlet radius, and throat radius. The throat radius should be smaller than the outlet radius to ensure an uninterrupted flow of steam in the cooling tower. The throat radius's height is around two-thirds of the cooling tower's height. The tower outlet is indicated by red and white aircraft markings. Every construction that exceeds a certain height threshold must display aircraft markings to ensure the preservation of safe airspace [9]. The most vulnerable part of the cooling tower is the tower shell. The thickness of the shell is lower than 30cm, which makes the structure vulnerable to gusts of wind and seismic events [10-11]. The tower should periodically undergo a geometry control to prevent a collapse of the structure. Basic geometric control uses the total station to estimate the imperfection of tower geometry. Points are measured in vertical lines from a minimum of three positions. The limitation of the methods is the count of measured points. For detailed measurements, laser scanning is a suitable method, whose precision is similar to total station. Laser scanning is faster and gives more data on tower conditions for further analysis [12-16]. High humidity is not a suitable environment for reinforced concrete. Cooling tower shells degrade during years of operation. Humidity from the cooling process precipitates on the inner tower shell and it is looking for the easiest way out. When a crack in the tower shell appears, humidity flows through the material and reinforcement steel bars to corrode. Over time, corrosion begins to spread along the iron, leading to the expansion of the crack. More humidity starts to flow into the crack and stays there. In the last step, the size of a crack causes detachment of the concrete's part and the cavity creation. The structural integrity of the tower shell is compromised, posing a threat to the vicinity of the cooling tower and its operational stability [17].

Detection of damage caused by humidity is important to stop spreading of the corrosion along reinforced steel. Companies which provide cooling tower maintenance use visual control of damage from the ground by binoculars. This method does not provide accurate results. There are several solutions for damage detection and the first is the localisation of damage by laser scanning. Damage with concrete detachment is detectable by local curvature estimation [18]. Another approach involves employing thermography to identify alterations in concrete materials, such as structural damage [19]. An alternative for detecting damage by laser scanning is photogrammetry [20-21]. UAVs increase data availability from the above. It is not possible to take sufficient resolution from images by terrestrial photogrammetry. The UAV is used to record the entire tower shell even at height [22].

It is essential to provide a summary of cooling tower shell damage for the effective management of building ageing, particularly in terms of financing requirements. Damage is classified into several types: low damage/crack, high damage without reinforcement steel and high damage with reinforcement steel. High damage can be detected on Terrestrial laser scanning (TLS) data, low damage is hard to detect by TLS and close-range photogrammetry is needed. Crack detection algorithms can detect low damage, but tower shells contain several patterns, resembling cracks, including air pores, ribbing and formwork [23]. Mostly used are edge detectors like Sobel or Canny for crack detection, but when dealing with noisy image, which shares similar patterns, the task becomes more challenging. To improve the accuracy of detection cracks, the input images must be pre-processed by filters or change the colour space to HSI [24]. Another approach used RANdom SAmple Consensus (RANSAC) to detect lines on images and classified lines by Random Forest algorithm to crack and other patterns [25].

Currently, machine learning is predominantly used for detection tasks. Mandatory to use are convolution neural networks (CNN) or fully convolutional networks (FCN) with pre-trained models like VGG16 or ResNet [26]. To improve segmentation, U-NET design models CrackUnet [27-28].

The solution for low damage detection should be using multiple textures from processing images and laser scans in photogrammetric software. Textures like diffuse, normal, displacement and occlusion used in renderings technique contain important information on tower shell geometry.

Combining colour and geometric information in the same data format eliminates data preparation. The focus of this article revolves around utilising textures for detection in the field of civil engineering.

METHODS

Testing data

This article utilised data from a conference paper - Cooling tower measurement by laser scanner and close-range photogrammetry [17]. The following information pertains to the ITTERSON 100m cooling tower, which is the type designed by the Czech company ARMABETON Praha. The tower's height is 100 metres, and its shell is shaped like a rotating hyperbola. The tower shell starts at 5 metres and extends to 100 metres, with an inlet radius of 28.5 metres and an outlet radius of 18.17 metres. The analysis relied on a high-resolution mesh model of the cooling tower, obtained through laser scanning and photogrammetry. This detailed model captured textural information with a resolution of 3 mm per pixel, enabling precise damage detection.

$$\frac{x^2}{a^2} + \frac{y^2}{a^2} - \frac{z^2}{c^2} = 1 \tag{1}$$

The cooling tower was measured by laser scanning and photogrammetry for the calculation of a detailed mesh model with texture. The interface of aerial markings and columns of the cooling tower is located at the interfaces between the laser scans and the RGB images. Input for this article was a detailed mesh model of the cooling tower with 3mm/px texture resolution.

Projection

The textures of the mesh model were united into a map projection. A similar approach was used for laser scanning data to estimate the difference between mathematical model and measured model of cooling tower [29-30]. Cooling towers can be divided according to meridians and parallels, parallel are horizontal lines of circuit and meridians are vertical lines of height.
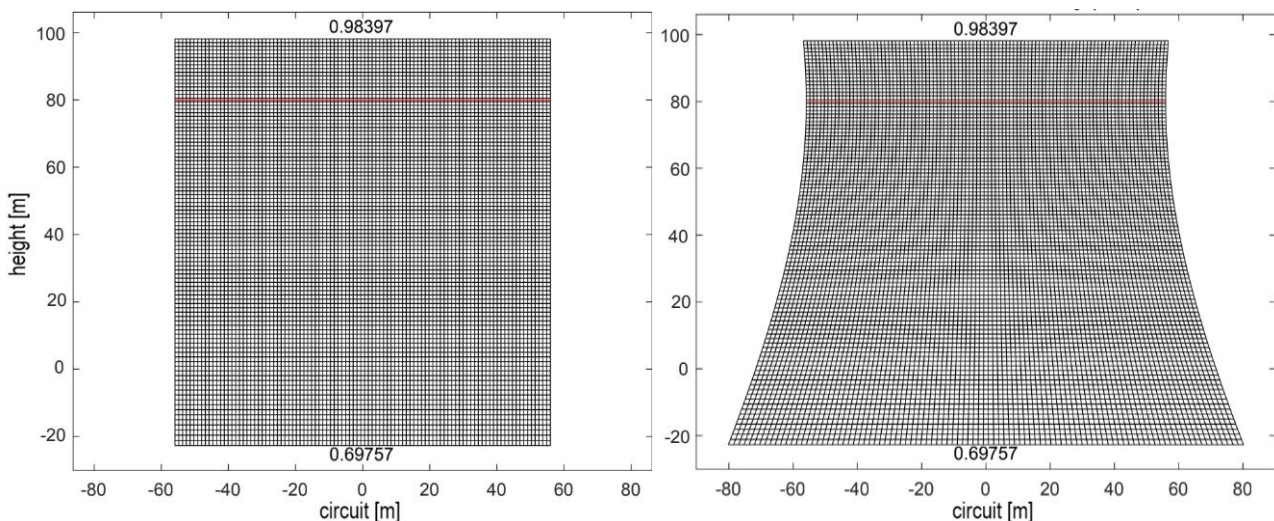

Fig. 1 – Textures (diffuse, normal, displacement, occlusion)

A cylindrical projection with one undistorted parallel was used for projecting hyperboloid onto a plane. For the projection, these are goniometric functions, where α is an angle which has the same meaning as the latitude. In this case, it is an angular distance between the undistorted parallel and any chosen parallel.

$$x = cosh(\alpha) \tag{2}$$

$$y = sinh(\alpha) \tag{3}$$

Mathematical model of the cooling tower was modelled in Blender Software [31] with edited UV maps of texture with descriptive projection. Texture projection was produced by Agisoft Metashape [32] from high detail model to mathematical model.

Textures

The sub-goal of this article is to utilise textures commonly used in rendering techniques to enhance detection in the field of civil engineering. Diffuse texture is used to define the base colour of an object. It is also known as the albedo map. The diffuse map is responsible for the colour of the object when it is not affected by any lighting conditions. Lighting conditions during the capture of input images impact the diffuse texture in photogrammetry if de-lighter software is not used. Normal texture is used to provide the perception of depth on a flat surface. It is used to add small details to the surface of an object without changing the geometry of the object. The normal map is created by using a high-resolution model and then transferring the surface details to a low-resolution model. The purpose of displacement texture is to enhance the three-dimensional appearance of an object's surface. It is used to create the illusion of geometry that is not present in the model. The displacement map is created by using a high-resolution model and then transferring the surface details to a low-resolution model. In the field of photogrammetry, a displacement texture is analogous to a Digital Elevation Model (DEM), except it is derived from a distinct foundational model rather than a flat plane. An occlusion texture is employed to replicate the phenomenon of shadowing that arises when two objects are close to one another. It is employed to enhance the three-dimensional appearance of the shadows and indentations on an item. [33] These textures are visible on Figure 2.
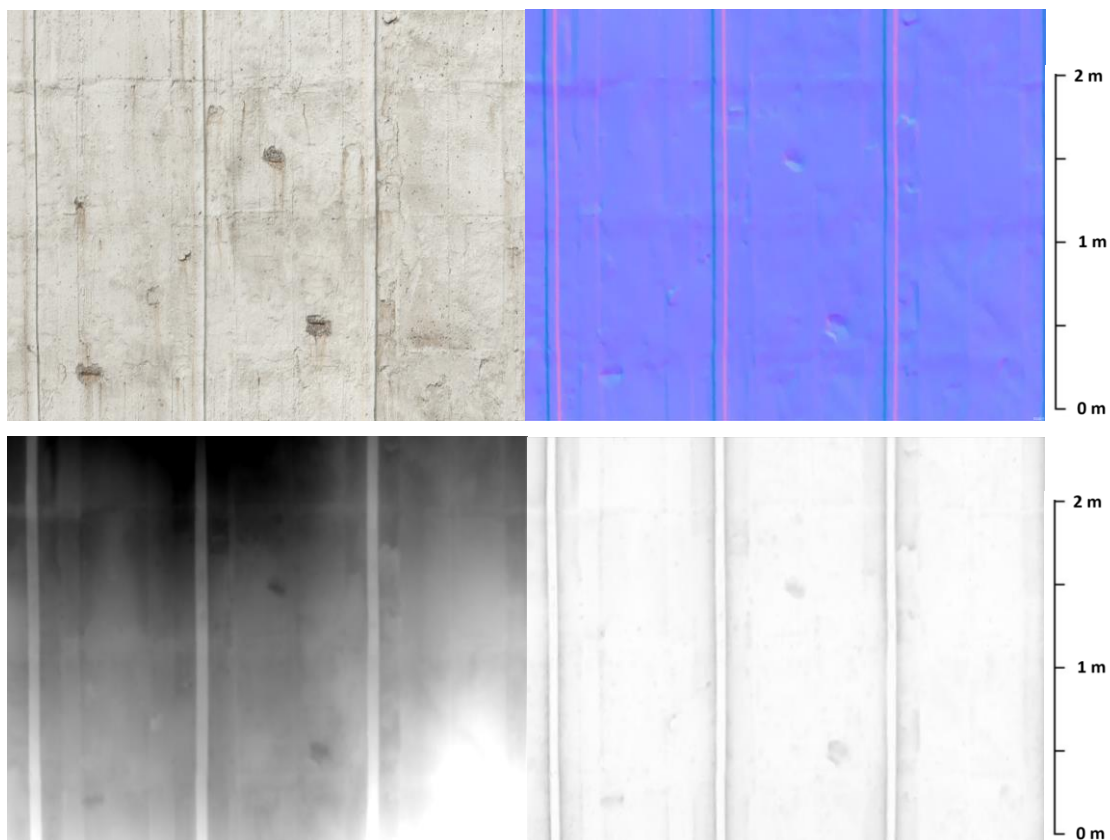

Fig. 2 – Textures (diffuse, normal, displacement, occlusion)

The intriguing texture is the normal texture. The texture consists of three bands that carry X, Y, and Z values of the normal vector visible on Figure 3. The normal vector values from the high-resolution model are recorded as pixel values in a normal texture. In the figure below, it is visible that the Y band eliminates the ribbing on concrete. This effect is achieved by aligned ribbing with a coordinate system of normals, which is helpful for the detection of ribbing.
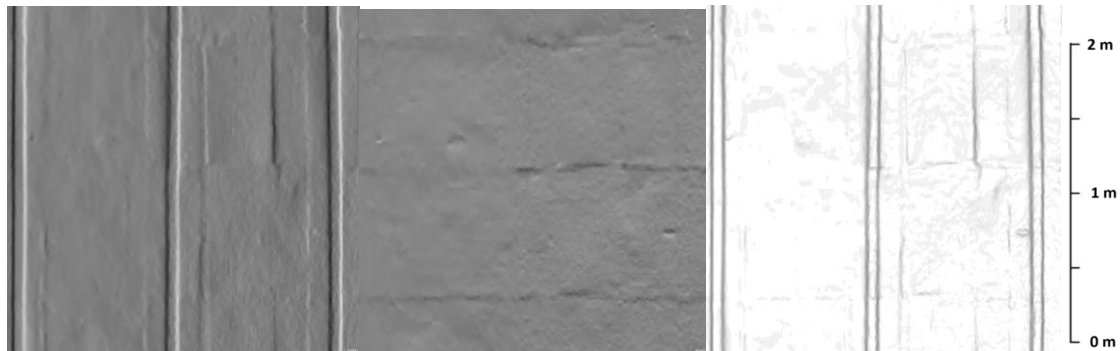

Fig. 3 – Normal texture - x (left), y (middle) and z (right)

RESULTS

The goal of the research was the automatic detection of damaged concrete on the tower shell. Damage is categorised into 4 categories visible in Figure 4: fine concrete, low damage, high damage without reinforcement and high damage with reinforcement. The key characteristics defining damage in the sustainability lifecycle of a cooling tower include the area, depth, volume, and length of visible reinforcement.
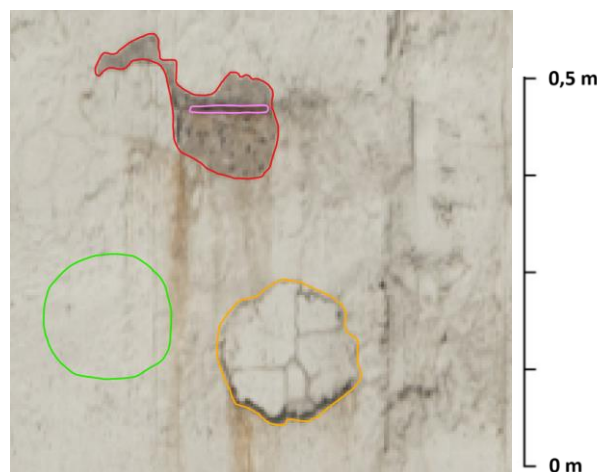

Fig. 4 – Red - high damage, pink - steel reinforcement, yellow - low damage, green - concrete

Detect high damage

Identifying extensive damage poses the least challenging aspect of the detection process. High damage is characterised by disturbed concrete with a different colour than fine concrete. For detection, diffuse texture (RGB) was used as the input layer for CNN in eCognition software version 10.3. Samples were created in QGIS as polygon objects with type attributes: concrete, low and high. Table1.

Tab. 1 - Summarization of samples

Type	Sum of samples
Concrete	40
Low damage	30
High damage	50

Across polygons, samples were created with augmentation multiplying samples 10 times. It was used for rotation, horizontal and vertical flip and zoom, this created many samples in Table 2. Size of the polygon concrete type was larger than other categories. The size of the samples was 32px.

Tab. 2 - Summarization of samples

Type	Sum of samples
Concrete	46150
Low damage	1420
High damage	2430

The Convolutional Neural Network contained 2 hidden layers. The kernel of the first layer was set at 7 and the number of distinct feature maps was 12. The kernel of the second layer was set to 5. CNN was trained by a 0.0006 learning rate, with 5000 training steps and 50 samples were used in each training step. Applying CNN heat maps with probabilities of occurrence of wanted objects were created. The raster layer was multi-resolution segmentation by Object-based image analysis (OBIA) with each layer (RGB texture and heatmaps). Generated objects were classified by heatmap values. Objects with the same classification were merged visible on Figure 5.

Fig. 5 – Detected High damage

Extract ribbing

Ribbing on tower shells is a disruptive element for low damage detection. Vertical edges of ribbing are similar to cracks of low damage. Meanwhile, testing detection of low damage with CNN was found to require the elimination of ribbing, for detection of ribbing CNN was used with the same design as in High damage detection. It was compared to the input layer to CNN: diffuse and normal texture visible on Figure 6. Polygons for sample creation were identical. For sample augmentation: horizontal flip and zoom. Rotation and vertical flip are unwanted due to ribbing orientation.
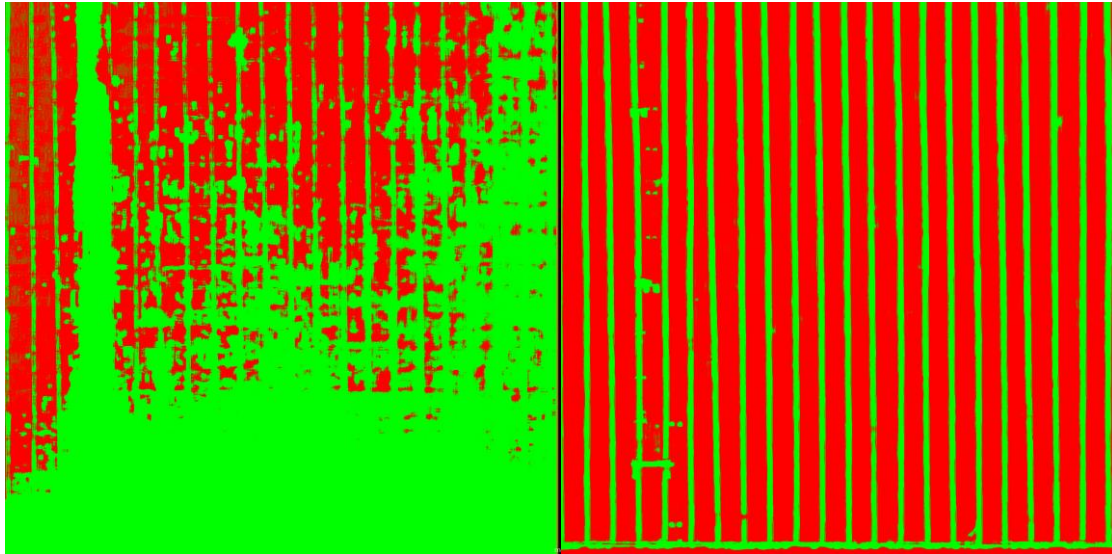

Fig. 6 – Classified concrete ribbing from diffuse (left), from normal (right)

Detect low damage

Low damage detection is the most challenging part. There are a lot of patterns on tower shells similar to cracks of low damage like air pores, edges of concrete formwork, ribbing and colour changes. Separating these patterns on diffuse texture (RGB) from crack is a hard task. In Figure 7 below is visible CNN detection of low damage on diffuse texture and composed raster layer. Detecting low damage based on diffuse texture is insufficient, to improve detection and eliminate unwanted patterns, a composed raster layer was created.
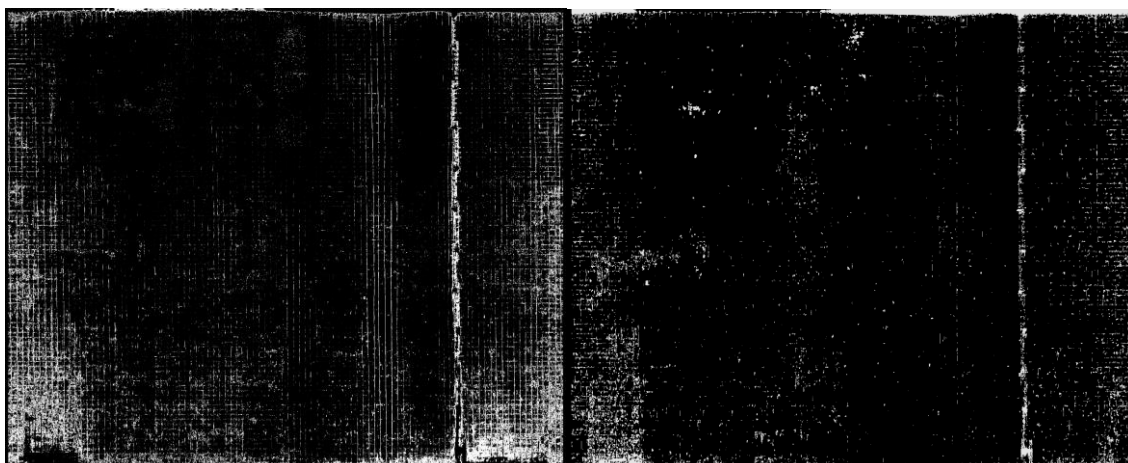

Fig. 7 – Heatmap of classified Low damage (from diffuse texture - left, from composed raster layer - right)

The composed raster layer is based on diffuse texture, normal texture, and displacement texture. The diffuse texture was converted from RGB to HSI colour space. An intensity band from HSI was used for further processing. From normal texture were used only bands with y values - normal Y. Displacement texture containing values from -20cm to 20cm, which is not suitable for slope estimation, so displacement texture was multiplied 1000x times to increase values to prevent numerical errors. Each raster is visible on Figure 8.
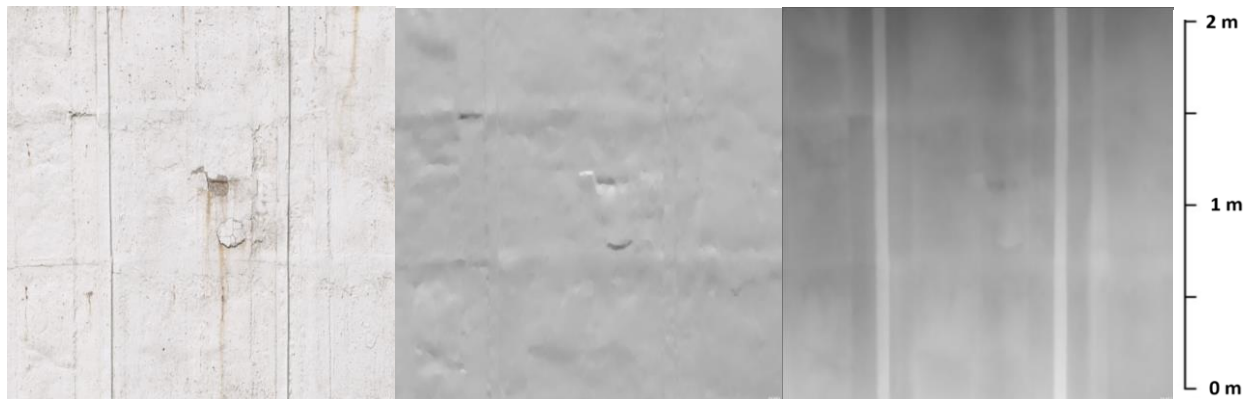

Fig. 8 – (input - diffuse, normal y, displacement)

The intensity layer and normal Y were processed by the Ridge filter to highlight raster edges. The kernel of the Ridge filter was set to size 3. The slope raster is calculated from multiplied displacement texture visible on Figure 9.
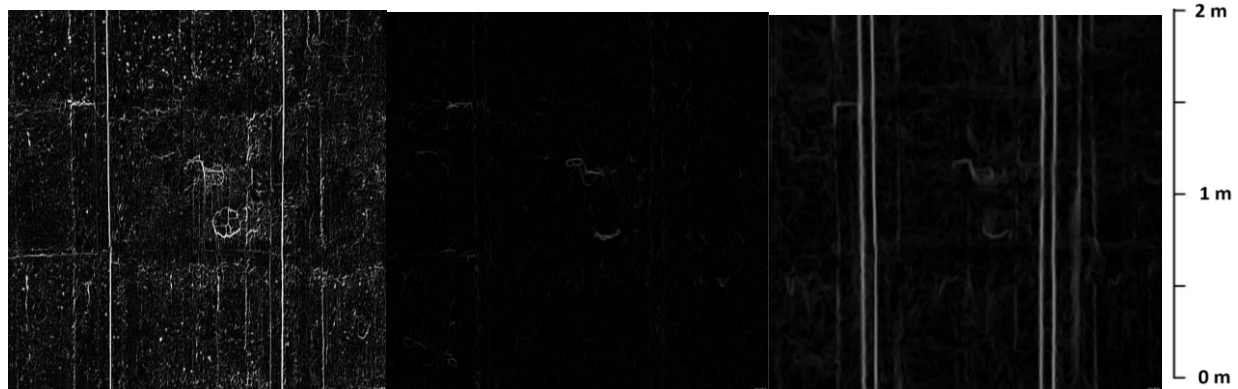

Fig. 9 – (Intensity ridge filter, normal Y ridge filter, slope)

Layers with highlighted edges were joined together with the same weight and blurred by a median filter to remove air pores. The final raster layer is composed of the Intensity band and the blurred band visible on Figure 10.
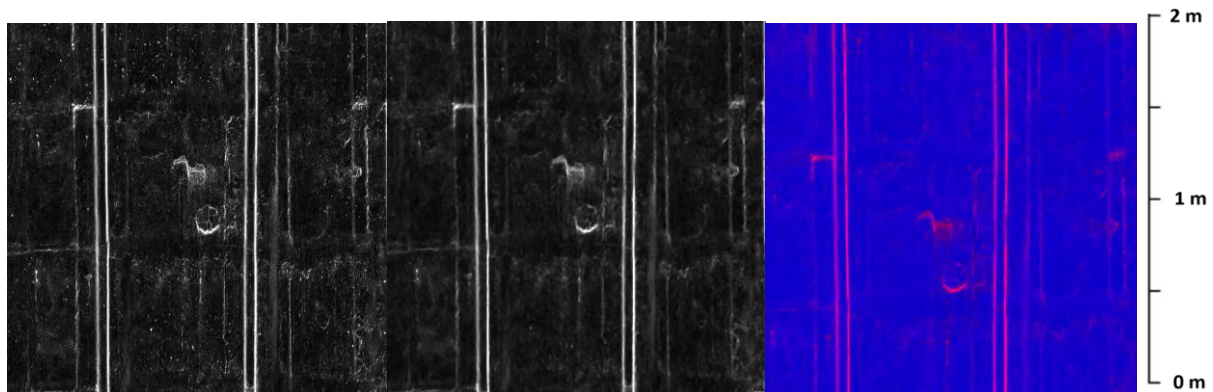
Fig. 10 – (summarization of highlight edges raster, median blur filter, composed raster layer)

The composed raster layer is used for multi-resolution segmentation by OBIA in eCognition software. The scale parameter was set to default on value 42. The shape parameter was set to 0.2 and compactness 0.7. Created objects were classified by rules in Table 3 below into 4 categories: fine concrete, ribbing, low and high damage visible on Figure 11.

Tab. 3 - Classification rules

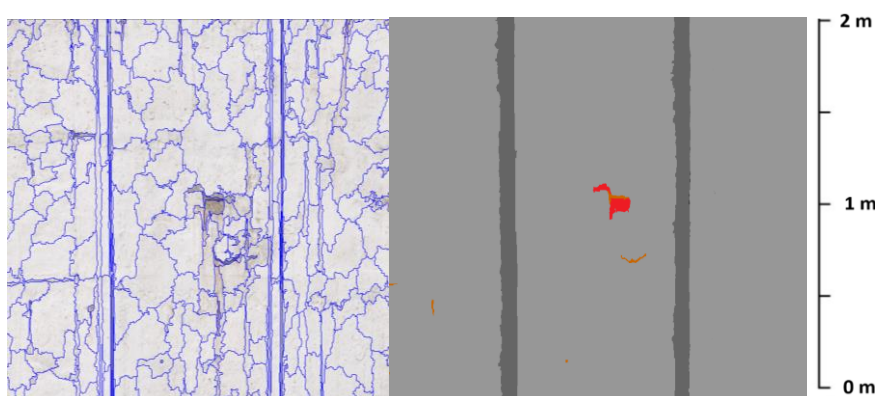|	Fine concrete	Ribbing	High Damage	Low damage
CNN Heatmap ribbing	<0.9	>0.9	<0.9	<0.9
CNN Heatmap high damage	<0.9	-	>0.9	<0.9
Blurred band	<median(blur)	-	>median(blur)	>median(blur)

Fig. 11 – (segmented objects - left, classified object - right)

The volume of high damage

Estimation of missing concrete volume is processed by pixel summarization like on DEM. On the contrary, DEM utilises displacement texture, assigning values based on the disparity between the actual geometry and the design geometry. Volume is estimated by summarization of pixel values on high-damage objects reduced by mass given by a boundary-like fitting plane on the boundary. Example of estimation of missing concrete is visible on Figure 12, 13.

$$V = (\Sigma(pixel\ value\ inside \times pixel\ resolution^2) - \frac{\Sigma(pixel\ value\ boundary)}{n} \times S) \times m_p \qquad (4)$$
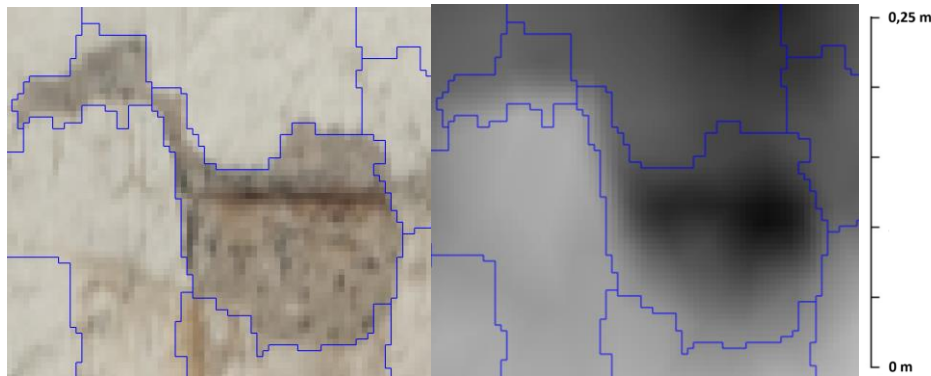

Fig. 12 – high damage on diffuse (left) and displacement texture (right)

Fig. 13 – (examples of detected low damage)

CONCLUSION

Damage classification and summarization on cooling tower shells is an integral part of controlling the ageing of buildings and structures. During the lifecycle of the cooling tower, the shell is damaged and needs repairs. Damages are classified into low damage/ cracks, high damage without visible reinforcement steel and high damage with reinforcement steel The proposed method of detecting damage is based on data from laser scanning and close-range photogrammetry by UAV. A mesh model with several types of textures (diffuse, normal, displacement and occlusion) is created by measured point clouds and images.

Textures are modified to map projection to view the entire tower shell in one raster. The mathematical model of the hyperbolic cooling tower was modelled in Blender software which defines UV maps for projection. It used cylindrical projection with one not distorted axis. Based on the mathematical model diffuse, normal, displacement and occlusion textures were generated. Each texture was used in damage detection except for the occlusion texture. Occlusion texture provides information about the visualisation of shadow, similar information is also on normal and displacement texture.

Detecting high damage was done by CNN in eCognition software. Training samples were created by manual vectorization on part of the tower shell. All high damages were detected with misdetection on the ladder and shadows area. Misdetection was caused by a low number of samples

and labels of samples. eCognition uses labels in the form of labels for one sample, in some cases this leads to an inaccurate CNN model. High damages are not aligned with image coordinates, which leads to label samples which contain damage and fine concrete.

The tower shell is full of patterns similar to low damages/cracks like air pores, ribbing, formwork and change colour. Detecting low damage only on diffuse texture by CNN was insufficient. For detection of low damage, a pre-processed composed raster layer based on diffuse, normal and displacement texture. The composed raster layer increases low damage based on colour and geometry, which helps to separate low damage from other patterns. The Tower shell was segmented by multiresolution segmentation and classified by composed raster layer and additional rules. This method leads to low accuracy detection of low damage. The position of low damage is precise, but the damage is typically not inaccurately marked.

The successful usefulness of textures from rendering techniques has been demonstrated for damage detection and cooling tower shells. The study was limited by only one measured cooling tower and selection of eCognitions software for damage detection. Easy usage of CNN inside commercial software minimises options for optimization of detection methods. Future work will focus on different machine learning models like U-NET for low damage detection. Also adding thermography during right weather conditions may help improve detection of low damage. Low damage is a piece of concrete which is detached from the tower shell and its temperature capacity will be different.

The demonstrated method for evaluating damage on cooling towers offers practical benefits in localising and summarising damage, aiding operators in repair planning and decision-making processes. Utilising drone-based visual inspection proves to be a cost-effective alternative to employing professional climbers, significantly reducing inspection time. While measurements by drones are completed within 6 hours, the conventional approach with climbers can take several days to inspect all tower shells. The collected data from drone inspections not only facilitate immediate repair planning but also serve as valuable input for future predictive maintenance through periodic measurements. By leveraging this data, operators can anticipate potential damage trends and prioritise maintenance efforts, accordingly, ultimately optimising the lifespan and performance of cooling tower structures. The method can also be used on other concrete structures (bridges, silos, dams).

ACKNOWLEDGEMENTS

REFERENCES

[1]   Berra, E. F. & Peppa, M. V. 2020. Advances and challenges of UAV SFM MVS photogrammetry and remote sensing: Short review. (2020) IEEE Latin American GRSS & ISPRS remote sensing conference (lagirs) (pp. 533-538). IEEE.

[2]   Pavelka, K., Hůlková, M., Šedina & J., Pavelka, K. 2019. RPAS for documentation of Nazca aqueducts European Journal of Remote Sensing. (2019), 52(1), 174-181. ISSN 2279-7254. https://doi.org/10.1080/22797254.2018.1490321

[3]   Bouček, T., Stará, L., Pavelka, K. & Pavelka, K., Jr. 2023. Monitoring of the Rehabilitation of the Historic World War II US Air Force Base in Greenland. Remote Sens. 2023, 15, 4323. https://doi.org/10.3390/rs15174323

[4]   Marčiš, M.; Fraštia, M.; Kovanič, Ľ.; Blišťan, P. 2023. Deformations of Image Blocks in Photogrammetric Documentation of Cultural Heritage—Case Study: Saint James's Chapel in Bratislava, Slovakia. Appl. Sci. 2023, 13, 261. https://doi.org/10.3390/app13010261

[5]   Štroner, M., Urban, R., Seidl, J., Reindl, T. & Brouček, J. 2021. Photogrammetry using UAV-mounted GNSS RTK: Georeferencing strategies without GCPs. Remote Sensing (2021), 13(7), 1336. https://doi.org/10.3390/rs13071336

[6]   Štroner, M., Urban, R., Reindl, T., Seidl, J. & Brouček, J. 2020. Evaluation of the georeferencing accuracy of a photogrammetric model using a quadrocopter with onboard GNSS RTK. Sensors (2020), 20(8), 2318. https://doi.org/10.3390/s20082318

[7]   Asadzadeh E. & Alam M. 2014. A survey on hyperbolic cooling towers., International Journal of Civil, Environmental, Structural, Construction and Architectural Engineering 8, 1079-1091 (2014).

[8]   Gupta, A. K., & Maestrini, S. 1986. Investigation on hyperbolic cooling tower ultimate behaviour. Engineering Structures, 8(2), 87-92. https://doi.org/10.1016/0013-7944(86)90012-1

[9]   Kraetzig W. B., et al. 2009. From large natural draft cooling tower shells to chimneys of solar upwind power plants., Symposium of the International Association for Shell and Spatial Structures (2009).

[10]   Hara, T. & Gould, P. L. 2003. Local–global analysis of cooling tower with cutouts, Computers & structures 80.27-30, 2157-2166. https://doi.org/10.1016/S0045-7949(02)00250-X

[11]   Kulkarni S. & Kulkarni A. V., 2014. Case study of seismic effect on hyperbolic cooling towers. Civil Environ. Res 6.11, 85-94 (2014).

[12]   Głowacki, T., Muszyński, Z. 2018. Analysis of cooling tower's geometry by means of geodetic and thermovision method IOP Conf. Ser.: Mater. Sci. Eng. 365 042075, https://doi.org/10.1088/1757-899X/365/4/042075

[13]   Głowacki T., Grzempowski P., Sudoł E., Wajs J. & Zając M., 2016, The assessment of the application of terrestrial laser scanning for measuring the geometrics of cooling towers, Geomatics, Landmanagement and Landscape, 4, 49–57 (2016).

[14]   Bajtala M., et al. 2011. Exploitation of Terrestrial Laser Scanning in Determining of Geometry of a Factory Chimney., Proceedings of the 5th International Conference on Engineering Surveying (INGEO 2011). Brijuni, Croatia, September. (2011).

[15]   Pandžić J., et al. 2016, TLS in determining geometry of a tall structure. Engineering geodesy for construction works, industry and research, proceedings of the international symposium on engineering geodesy. (2016).

[16]   Kocierz R., Rębisz M. & Ortyl L., 2018. Measurement points density and measurement methods in determining the geometric imperfections of shell surfaces., Reports on Geodesy and Geoinformatics 105 (2018).

[17]   Zahradník, D. 2023. Cooling tower measurement by laser scanner and close-range photogrammetry. AIP Conference Proceedings (Vol. 2928, No. 1). AIP Publishing https://doi.org/10.1063/5.0079223

[18]   Makuch M. & Gawronek P. 2020. 3D point cloud analysis for damage detection on hyperboloid cooling tower shells, Remote Sensing 12.10 1542 (2020). https://doi.org/10.3390/rs12101542

[19]   Głowacki T. & Muszyński Z. 2018 Analysis of cooling tower's geometry by means of geodetic and thermovision method, IOP Conference Series: Materials Science and Engineering. Vol. 365. No. 4. IOP Publishing (2018).

[20]   Chisholm N. W. T. 1997. Photogrammetry for cooling tower shape surveys. The Photogrammetric Record 9.50 173-191 (1977).

[21]   Ioannidis, C., Valani, A., Soile, S., Tsiligiris, E. & Georgopoulos, A. 2007. Alternative techniques for the creation of 3D models for finite element analysis—Application on a cooling tower. Proc. Opt. https://doi.org/10.13140/2.1.5124.2887

[22]   Castiglioni, C. A., Rabuffetti, A. S., Chiarelli, G. P., Brambilla, G., & Georgi, J. 2017. Unmanned aerial vehicle (UAV) application to the structural health assessment of large civil engineering structures. In Fifth International Conference on Remote Sensing and Geoinformation of the Environment (RSCy2017) (Vol. 10444, pp. 355-370). SPIE.

[23]   Fujita, Y., Mitani, Y., & Hamamoto, Y. 2006. A method for crack detection on a concrete structure. In 18th International Conference on Pattern Recognition (ICPR'06) (Vol. 3, pp. 901-904). IEEE.

[24]   Nnolim, U. A. 2020. Automated crack segmentation via saturation channel thresholding, area classification and fusion of modified level set segmentation with Canny edge detection. Heliyon, 6(12). https://doi.org/10.1016/j.heliyon.2020.e05748

[25]   Prasanna, P., Dana, K. J., Gucunski, N., Basily, B. B., La, H. M., Lim, R. S. & Parvardeh, H. 2014. Automated crack detection on concrete bridges. IEEE Transactions on automation science and engineering, 13(2), 591-599.

[26]   Dung, C. V. 2019. Autonomous concrete crack detection using deep fully convolutional neural network. Automation in Construction, 99, 52-58.

[27]   Zhang, L., Shen, J. & Zhu, B. 2021. A research on an improved Unet-based concrete crack detection algorithm. Structural Health Monitoring, 20(4), 1864-1879.

[28]   Liu, Z., Cao, Y., Wang, Y. & Wang, W. 2019. Computer vision-based concrete crack detection using U-net fully convolutional networks. Automation in Construction, 104, 129-139.

[29]   Kwinta A. and Bac-Bronowicz J., 2021. Analysis of hyperboloid cooling tower projection on 2D shape, Geomatics, Landmanagement and Landscape (2021).

[30]   Beshr, A. A., Basha, A. M., El-Madany, S. A. & El-Azeem, F. A. 2023, Deformation of High-Rise Cooling Tower through Projection of Coordinates Resulted from Terrestrial Laser Scanner Observations onto a Vertical Plane. ISPRS International Journal of Geo-Information, 12(10), 417. https://doi.org/10.3390/ijgi12100417

[31]   blender.org - Home of the Blender project - Free and Open 3D Creation Software. (n.d.). blender.org. https://www.blender.org/ (cited 30-3-2024)

[32]   Agisoft Metashape: https://www.agisoft.com/ (cited 30-3-2024)

[33]   Texture Maps Explained | Poliigon Help Center. (n.d.). https://help.poliigon.com/en/articles/1712652-texture-maps-explained (cited 30-3-2024)